A multi-mode low ripple charge pump with active regulation*

Ye Qiang(叶强)†, Lai Xinquan(来新泉)†, Xu Luping(许录平), Wang Hui(王辉), Zeng Huali(曾华丽), and Chen Fuji(陈富吉)

(Institute of Electronic CAD, Xidian University, Xi'an 710071, China)

Abstract: In order to improve efficiency and reduce the output ripple, a novel multi-mode charge pump is presented. The proposed charge pump includes dual-loop regulation topology-skip and linear modes. It consumes low quiescent current in skip mode for light loads, and produces low ripple in linear mode for heavy loads, which closes the gap between linear mode and skip mode with active regulation; a multi-mode charge pump employing the technique has been implemented in the UMC 0.6-μm-BCD process. The results indicate that the charge pump works well and effectively; it has low ripple with special regulation, and minimizes the size of the capacitance, then decreases the area of the PCB board. The adjustable output of the positive charge pump is 10–30 V, and the maximum output ripple is 100 mV when the load current is 200 mA. The line regulation is 0.2%/V, and load regulation is 0.075%.

Key words: charge pump; multi-mode; low ripple; low consumption
DOI: 10.1088/1674-4926/30/12/125006 **EEACC:** 2570P; 2570A; 2560P

1. Introduction

In medium and small power charge pump switched power supplies, the multi-mode controlling technique in closed loop feedback controlling systems, which achieves better dynamic performance, higher precision, larger gain bandwidth and protection from transient large current, is widely utilized.

The electrical equipment needs a specific operating voltage with low ripple and good line regulation as well as good load regulation, therefore a multi-mode efficient charge pump with low output ripple and low quiescent current is presented in this paper. Compared with the traditional charge pump, the proposed circuit can produce a very low output ripple with special regulation in linear mode for heavy loads, and consumes very low quiescent current in skip mode for light loads. The charge pump can work well and effectively, occupies a small PCB board space, radiates low EMI and offers high efficiency. It can compete with inductive converters when the input voltage is supplied with battery powered systems.

The paper presents a multi-mode charge pump regulation technique and circuit, which include skip mode and linear mode. It achieves low output ripple and low power dissipation. The testing results show that the charge pump works stably and effectively.

2. Structure of multi-mode charge pump

Figure 1 shows the structure of the proposed charge pump, which consists of a dual loop regulation technique. It includes an error amplifier EA, a comparator, a V–I conversion circuit, a reference block REF, an oscillator and logic, a high side power switch driver bufferp, and a low side power switch driver buffern inside the chip. C_{pump} is a flying capacitor, C_{out} is an output capacitor, and D1 and D2 are charging and discharging diodes.

2.1. Realization of the proposed charge pump circuit

Figure 2 presents the proposed charge pump circuit. The error amplifier EA amplifies the error between VREF1 and VFB, and EAOUT is the output signal of EA. We make a $V-I$ transformation and superimpose it with the reference current I_{REF1}; the summation is I_{SUM}, so we can find that,

$$I_{\text{EA}} = \frac{V_{\text{EAOUT}} - V_{\text{GSM7}}}{R_2}, I_{\text{REF1}} = \frac{V_{\text{REF2}}}{R_3},\ I_{\text{REF2}} = \frac{V_{\text{GSM1}}}{R_1}, \quad (1)$$

$$I_{\text{SUM}} = K_2(K_1 I_{\text{EA}} + I_{\text{REF1}}) = \frac{(W/L)_{\text{M13}}}{(W/L)_{\text{M10}}}\left[I_{\text{REF1}} - \frac{(W/L)_{\text{M9}}}{(W/L)_{\text{M8}}} I_{\text{EA}}\right]. \quad (2)$$

The active regulation function can be expressed as:

$$F_{\text{MODE-SEL}} = K_4 I_{\text{SUM}} - K_3 I_{\text{REF2}} = \frac{(W/L)_{\text{M5}}}{(W/L)_{\text{M14}}} I_{\text{SUM}} - \frac{(W/L)_{\text{M25}}}{(W/L)_{\text{M2}}} I_{\text{REF2}}. \quad (3)$$

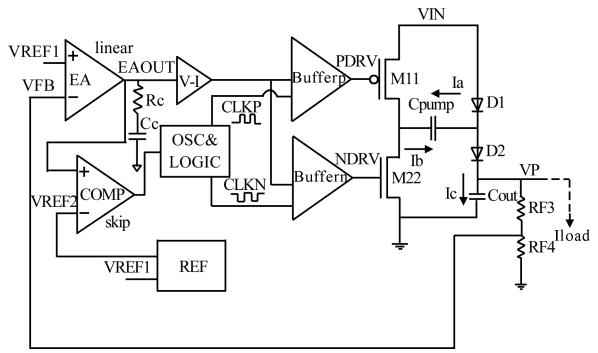

Fig. 1. Function block diagram of multi-mode.

* Project supported by the National Natural Science Foundation of China (No. 60876023).
† Corresponding author. Email: yeqiang4213@126.com, xqlai@mail.xidian.edu.cn
Received 26 May 2009, revised manuscript received 24 August 2009

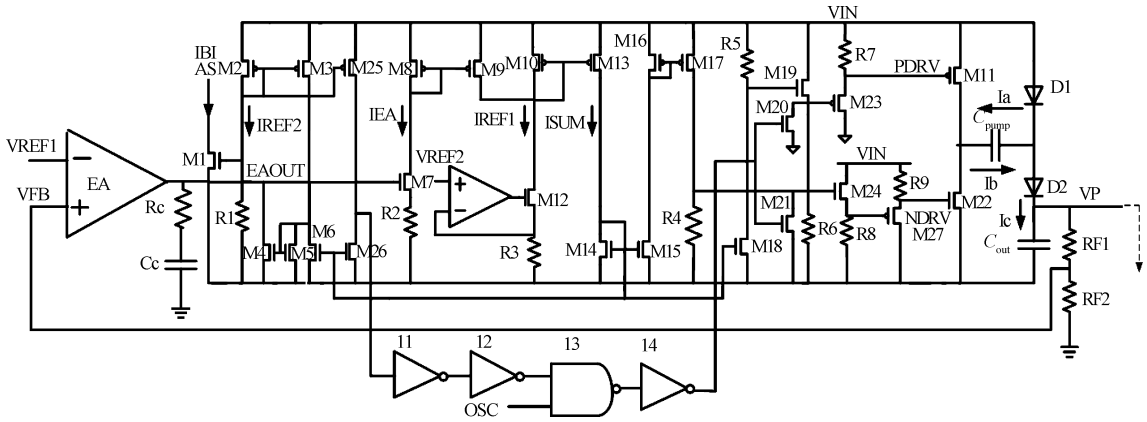

Fig. 2. Circuit of the proposed charge pump.

In Ref. [1], the charge pump regulates the turn on time of the power switches M3 and M4; in this paper the proposed charge pump can detect the load current by the feedback voltage $V_{\rm FB}$, regulate the turn on time in skip mode, and regulate $R_{\rm dson}$ of power switches M11and M22 in linear mode; the efficiency and output ripple has been improved. When the load is light, $V_{\rm FB}\uparrow$, $V_{\rm EAOUT}\uparrow$, $I_{\rm SUM}\downarrow$, if $F_{\rm MODE-SEL} < 0$, the charge pump enters into skip mode; when the load is heavy, $V_{\rm FB}\downarrow$, $V_{\rm EAOUT}\downarrow$, $I_{\rm SUM}\uparrow$, if $F_{\rm MODE-SEL} \geqslant 0$, the charge pump enters into linear mode, so, the proposed charge pump works effectively with active regulation.

For a light load, the charge pump enters into skip mode[1], which consumes low quiescent current, the output of I_4 is low, M20 and M21 turn off, so M11 turns on and M22 turns off. In the meanwhile, EAOUT is pulled down by M4, whose current is determined by $I_{\rm sum}$ and $I_{\rm REF2}$. When $I_{\rm sum}$ is less than $K_3 I_{\rm REF2}$, the output of I4 is high, M20 and M21 turn on, therefore M11 turns on, M22 turns off, and EAOUT is pulled up by M3 at the moment. The actual process can be divided into two states, charging state and discharging state.

Charging state: D1 and M22 turn on, $C_{\rm pump}$ is charged[2, 3], charging current is $I_{\rm a}$, charging time is $t_{\rm ch}$, and the voltage across $C_{\rm pump}$ is $VC_{\rm pump}$. $C_{\rm out}$ supplies current to load; for the cycle n, the skip period is mT,

$$V_{\rm NDRV} = I_{\rm SUM}R_4 - V_{\rm GSM24} + V_{\rm GSM27} \approx I_{\rm SUM}R_4, \tag{4}$$

$$R_{\rm ONM22} = f(V_{\rm NDRV}) = \frac{\partial V_{\rm DSM22}}{\partial I_{\rm a}}, \tag{5}$$

$$I_{\rm a} = \frac{1}{2}u_{\rm n}c_{\rm ox}(I_{\rm SUM}R_4 - V_{\rm THN})^2, \tag{6}$$

$$VC_{\rm pump} = V_{\rm IN} - V_{\rm D1} - \frac{1}{2}u_{\rm n}c_{\rm ox}(I_{\rm SUM}R_4 - V_{\rm THN})^2 R_{\rm ONM22}, \tag{7}$$

$$I_{\rm C}[nT, nT + t_{\rm ch}] = -I_{\rm load}. \tag{8}$$

Discharging state: M11 and D2 turn on, $C_{\rm pump}$ discharges current and transfers energy from Cpump to $C_{\rm out}$, neglecting the dead time effects, the discharge time is $mT - t_{\rm ch}$, and $I_{\rm b}$ is discharging current, so

$$V_{\rm PDRV} = V_{\rm IN} - I_{\rm SUM}R_5 - V_{\rm GSM19} + V_{\rm GSM23} \approx V_{\rm IN} - I_{\rm SUM}R_5, \tag{9}$$

$$R_{\rm ONM11} = f(V_{\rm NDRV}) = \frac{\partial V_{\rm DSM11}}{\partial I_{\rm b}}, \tag{10}$$

$$I_{\rm b} \approx \frac{1}{2}u_{\rm p}{\rm cox}(V_{\rm IN} - I_{\rm SUM}R_5 - V_{\rm THP})^2, \tag{11}$$

$$V_{\rm P} = V_{\rm IN} + VC_{\rm pump} - V_{\rm D2}, \\ -\frac{1}{2}u_{\rm p}{\rm cox}(V_{\rm IN} - I_{\rm SUM}R_5 - V_{\rm THP})^2 R_{\rm ONM11}, \tag{12}$$

$$I_{\rm C}[nT + t_{\rm ch}, (n+m)T] = \frac{mT}{mT - t_{\rm ch}}I_{\rm load}. \tag{13}$$

Since the transfer energy is constant, so

$$I_{\rm a}t_{\rm ch} = I_{\rm b}(mT - t_{\rm ch}), I_{\rm c}(mT - t_{\rm ch}) = I_{\rm load}mT. \tag{14}$$

From Eqs. (11) and (13), we find that

$$I_{\rm a} = \frac{mT - t_{\rm ch}}{t_{\rm ch}}I_{\rm b} = \frac{mT - t_{\rm ch}}{t_{\rm ch}}(I_{\rm c} + I_{\rm load}) = \frac{2mT - t_{\rm ch}}{t_{\rm ch}}I_{\rm load}. \tag{15}$$

Thus from Eqs. (10) and (14), we have

$$V_{\rm P} = 2V_{\rm IN} - (V_{\rm D1} + V_{\rm D2}) \\ - I_{\rm load}\left(\frac{2mT - t_{\rm ch}}{mT - t_{\rm ch}}R_{\rm ONM11} + \frac{2mT - t_{\rm ch}}{t_{\rm ch}}R_{\rm ONM22}\right). \tag{16}$$

The output ripple $V_{\rm PP}$ can be written as follows:

$$V_{\rm PP}({\rm skip}) = \frac{2mT - t_{\rm ch}}{mT - t_{\rm ch}}R_{\rm ESR}I_{\rm load} + \frac{mTI_{\rm load}}{C_{\rm out}}. \tag{17}$$

When the load is heavy, the charge pump regulates in linear mode, the amplifier amplifies the difference between feedback signal $V_{\rm FB}$ and $V_{\rm REF}$, and regulates the conductive resistance $R_{\rm DSON}$ of M11 and M22 to control the charging and discharging current, which work in saturation[4–6].

Charging state: D1 and M22 turn on, $C_{\rm pump}$ is charged, charging current is $I_{\rm a}$, charging time is $T/2$, and the voltage across $C_{\rm pump}$ is $VC_{\rm pump}$. $C_{\rm out}$ supplies current to load; for the cycle n, the clock period of OSC is T,

$$I_{\rm C}[nT, nT + t_{\rm ch}] = -I_{\rm load}. \tag{18}$$

Discharging state: M11 and D2 turn on, the $C_{\rm pump}$ discharges current and transfers energy from $C_{\rm pump}$ to $C_{\rm out}$, neglecting the dead time effects, and the discharge time is $T/2$, so

$$I_{\rm C}[nT + T/2, (n+1)T] = I_{\rm b} - I_{\rm load} = I_{\rm load}. \tag{19}$$

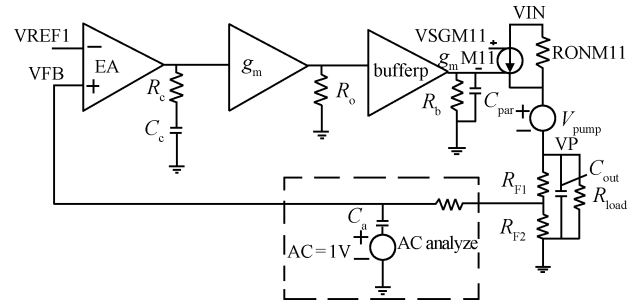

Fig. 3. Model for AC analysis of the charge pump.

Thus from Eqs. (4) and (12), V_P can be deduced as follows:

$$V_P = 2V_{IN} - 2I_{load}\sum_{N=1}^{2} R_{ONMNN} - \sum_{M=1}^{2} V_{DM}. \quad (20)$$

The output ripple of V_P can be calculated as:

$$V_{PP}(\text{linear}) = 2I_{load}R_{ESR} + I_{load}T/(2C_{out}). \quad (21)$$

For heavy loads, the charge pump operates in linear mode, and the output ripple is very low. For the cycle n, when $nT < t < nT + T/2$, OSC is high, so M11 turns on and M22 turns off. When $nT + T/2 < t < nT + T$, the corresponding state is that M11 turns off and M22 turns on, and it is evident that[7–9],

$$V_{PDRV} = \begin{cases} V_{IN} - I_{SUM}R_5, & nT < t < nT + T/2, \\ V_{IN}, & nT + T/2 < t < nT + T, \end{cases} \quad (22)$$

$$V_{NDRV} = \begin{cases} 0, & nT < t < nT + T/2, \\ I_{SUM}R_4, & nT + T/2 < t < nT + T. \end{cases} \quad (23)$$

2.2. Stability analysis of the charge pump in linear mode

Figure 3 shows the model for AC analysis of the charge pump; the error amplifier EA is realized through a traditional trans-conductance amplifier. R_C and C_C are the internal compensation resistance and capacitance. R_o is the output resistance of g_m-stage. R_b is the output impedance of bufferp, C_{par} is the parasitic capacitance of power switch M11, the voltage controlled current source is used for modeling gm of M11, and R_{ONM11} is the conduction resistance of M11. The voltage source V_{pump} is used for modeling C_{pump}. R_{F1} and R_{F2} is the feedback divided resistance, C_{out} is the output capacitance, and R_{load} is the load resistance. The voltage source, C_a and R_a in the dotted line block are used for AC small signal analysis.

From the above it is evident that when M11 turns on, the modulate loop has two poles within the crossover frequency, and one pole is far from the crossover frequency, so we can see that the transmission function can be expressed as:

$$H(s) = g_{mEA}R_{EA}g_mR_og_{mM11}(R_{ONM11}//R_{load})\frac{R_{F2}}{R_{F1}+R_{F2}} \times \frac{1 + s/R_CC_C}{[1 + s/(R_{EA}+R_C)C_C][1 + s/(R_{ONM11}//R_{load})C_{out}]}. \quad (24)$$

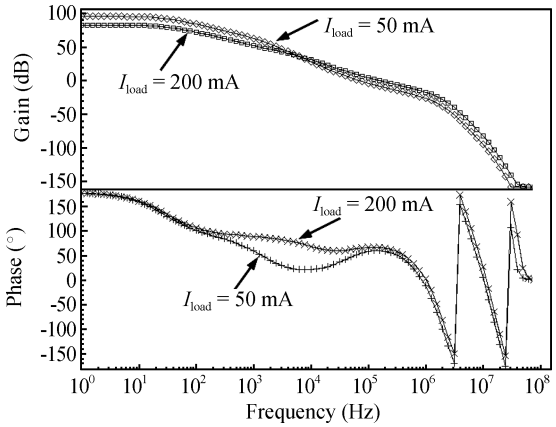

Fig. 4. Loop gain and phase versus frequency for different loads.

The dominant pole is:

$$f_{p1} = 1/2\pi(R_{EA} + R_C)C_C, \quad (25)$$

where R_{EA} is the output impedance of the error amplifier.

The non-dominant pole is:

$$f_{p2} = 1/2\pi(R_{ONM11}//R_{load})C_{out}. \quad (26)$$

The zero of compensation is:

$$f_z = 1/2\pi R_CC_C. \quad (27)$$

The DC open loop gain is:

$$A_V = g_{mEA}R_{EA}\frac{g_{mM7}}{1 + g_{mM7}R_2} \times R_5g_{mM11}(R_{ONM11}//R_{load})\frac{R_{F2}}{R_{F1}+R_{F2}}. \quad (28)$$

The parasitic pole is:

$$f_{par} = 1/2\pi C_{par}R_b. \quad (29)$$

The gain bandwidth product (GBW) is:

$$\text{GBW} = \frac{g_{mEA}g_{mM7}R_5g_{mM11}(R_{ONM11}//R_{load})}{2\pi C_{out}(1 + g_{mM7})}\frac{R_{F2}}{R_{F1}+R_{F2}}. \quad (30)$$

2.3. AC simulation results

Based on the UMC 0.6 μm-BCD process, the circuit is simulated using H-spice. Figure 4 presents the ac simulating results, and shows gain and phase versus frequency for I_{load} = 50 mA and I_{load} = 200 mA in linear mode. When I_{load} = 50 mA, the loop gain can be up to 96 dB, and phase margin is 60.2 °. When I_{load} is 200 mA, the loop gain is 83 dB, and phase margin is 66.9 °.The GBW is 164 kHz. When I_{load} varies from 0 to 200 mA, the load regulation is 0.075%.

3. Experimental results and microphotograph

Comparing skip mode with linear mode, the skip cycle is m, so the quiescent current I_q in linear mode is nearly m times in linear mode,

$$\frac{I_q(\text{skip})}{I_q(\text{linear})} \approx \frac{1}{m}. \quad (31)$$

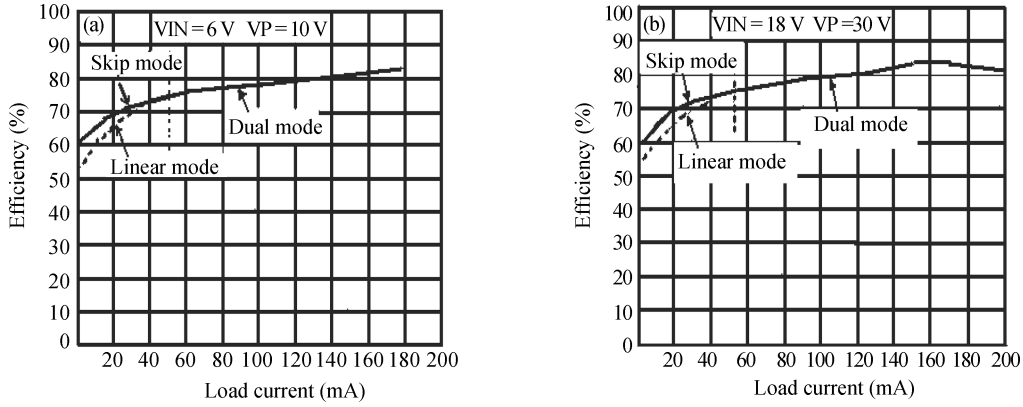

Fig. 5. Efficiency versus load current.

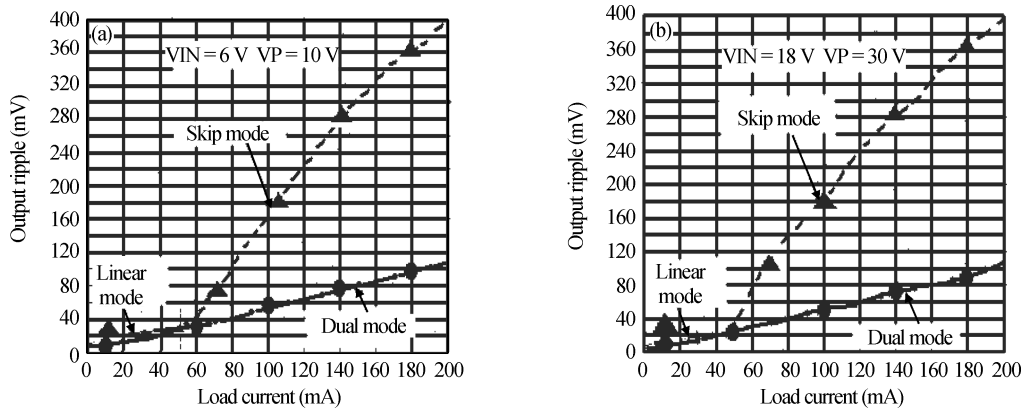

Fig. 6. Output ripple versus load current.

Neglecting the diode and power switch loss, the maximum efficiency is determined by power supply V_{IN} and output stage N, and the efficiency of the proposed multi-mode charge pump can be expressed as,

$$\eta = \frac{P_O}{P_{IN}} = \frac{V_P I_{LOAD}}{V_{IN} I_{IN}}, \quad \eta_{max} \approx \frac{V_P}{V_{IN} N}. \tag{32}$$

The proposed dual mode charge pump is used as a TFT LCD power supply, and the TFT LCD consumes about 0–200 mA power supply current; when the TFT LCD enters sleeping mode, the proposed charge pump works in skip mode and consumes a low power supply current, whose efficiency is higher than linear mode. When the TFT LCD is working in normal operation, the proposed charge pump can supply 200 mA current, which meets the low EMI and low power supply ripple application of TFT LCD.

Figures 5(a) and 5(b) show how the efficiency varies with load current. When $I_{load} < 50$ mA, the charge pump works in skip mode, which consumes a lower quiescent current than linear mode, so the efficiency for a light load is 8% higher than in linear mode. When $I_{load} \geqslant 50$ mA, the proposed charge pump works in linear mode. As the load varies from 0 to 200 mA, the maximum efficiency of the proposed charge pump can be up to 82.3%, so the proposed multi-mode charge pump for TFT LCD achieves high efficiency from a light load to a heavy load.

From Eqs. (17) and (21) we can find that

$$\frac{V_{PP}(\text{skip})}{V_{PP}(\text{linear})} = \frac{\dfrac{2mT - t_{ch}}{mT - t_{ch}} R_{ESR} I_{load} + \dfrac{mT I_{load}}{C_{out}}}{2 I_{load} R_{ESR} + I_{load} T/(2C_{out})} \approx 2m. \tag{33}$$

Figures 6(a) and 6(b) show the output ripple variation with load current. The output ripple is 15–400 mV in skip mode, and the output ripple is 12–104 mV, when the load current varies from 1 to 200 mA. When $I_{load} < 50$ mA, the proposed dual mode charge pump works in skip mode, and the output ripple is comparable with that in linear mode. When 50 mA $< I_{load} <$ 200 mA, the proposed charge pump works in linear mode, and the output ripple is reduced to 25% of the output ripple in skip mode. From Eqs. (17) and (21), it is obvious that the output cap C_{out} and operating frequency can reduce output ripple; the larger the cap and the higher the frequency are, the lower output ripple we can get. The output ripple is increased with the load.

Figures 7(a) and 7(b) are proposed charge pump waveforms when V_{IN} = 6 V, V_P = 10 V; Figures 7(c) and 7(d) are the waveforms when V_{IN} = 18 V, V_P = 30 V. The results show that the proposed charge pump works well in skip mode when the load is 40 mA, as well as in linear mode when the load is 100 mA, which is consistent with the curve of output ripple variation with load.

When a test and verification is made on the chip, the transient response is tested taking the output wave filtering capacitor C_{out} of 1 μF and the 100 mA square load current whose rising and falling times are 10 ns. We find that the output voltage pulse is in the range of 100 mV at the terminal V_P and there is no ringing in Fig. 8. Figure 9 is the microphotograph of the proposed charge pump; the area is 0.6025 mm^2.

Table 1 shows the proposed dual mode charge pump elec-

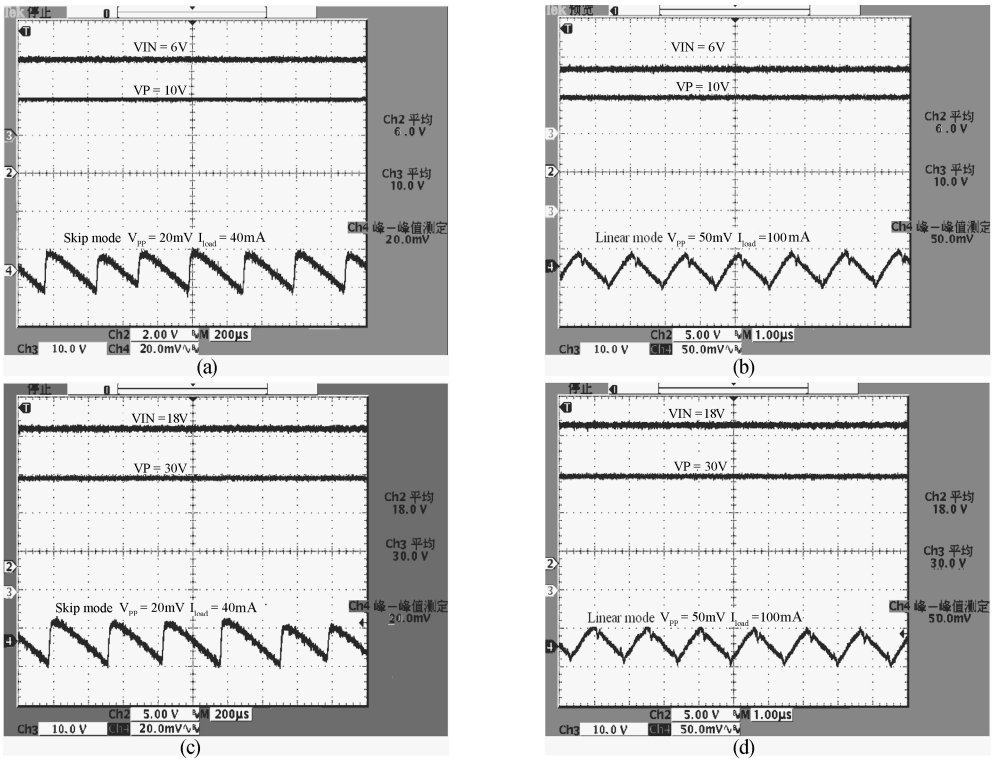

Fig. 7. Waveform of the proposed dual mode charge pump.

Fig. 8. Load transient response of the charge pump.

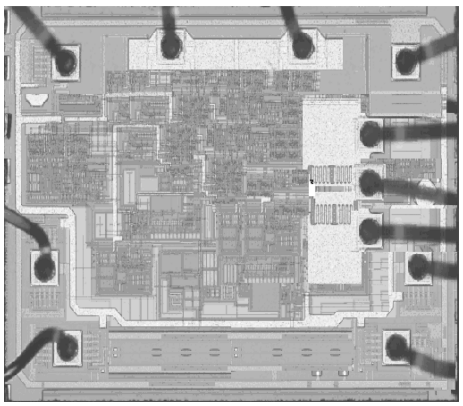

Fig. 9. Microphotograph of the charge pump.

Table 1. Comparison of the proposed dual mode charge pump with references.

Charge pump	Supply (V)	Output (V)	I_q (mA)	Ripple (mV/mA)	Maximum output current (mA)	Peak efficiency
This paper	6–18	10–30	0.4	0.5	200	82.3%
Ref. [1]	1.8–3.6	5	10	0.5	100	—
Ref. [4]	1.8	6.5	—	9	0.35	55%
Ref. [5]	1.6–2.4	2.22–2.31	—	—	8	94%

trical characteristics. When compared to Refs. [1, 4, 5], the proposed charge pump can supply more load current, and the output ripple is comparable with Ref. [1], although the peak efficiency is slightly lower than Ref. [5].

4. Conclusion

Based on the analyses of the multi-mode low ripple charge pump, it is shown that the proposed charge pump works well in skip mode for light loads, as well as in linear mode for heavy loads. The testing results show us that, while satisfying the system stability, the charge pump has a better transient response characteristic and load capacity, which produces low output ripple for heavy loads and consumes low quiescent current for light loads. It is suitable for low EMI and low cost systems, which occupy small PCB spaces.

References

[1] Bayer E, Schmeller H. Charge pump with active cycle

regulation-closing the gap between linear and skip modes. Proc IEEE Power Electron, 2000: 1497

[2] Dickson J F. On-chip high-voltage generation in NMOS integrated circuits using an improved voltage multiplier technique. IEEE J Solid-State Circuits, 1976, 11(6): 374

[3] Tanzawa T, Tanaka T. A dynamic analysis of the Dickson charge pump. IEEE J Solid-State Circuits, 1997, 32(8): 1231

[4] Pelliconi R, Iezzi D, Baroni A, et al. Power efficient charge pump in deep submicron standard CMOS technology. IEEE J Solid-State Circuits, 2003, 38(6): 1006

[5] Soldera J, Vilas Boas A, Olmos A. A low ripple fully integrated charge pump regulator. Integrated Circuits and Systems Design, 2003: 1777

[6] Gregoire B R. A compact switched-capacitor regulated charge pump power supply. IEEE J Solid-State Circuits, 2006, 8(41): 1944

[7] Zhao Hui, Xu Donglin, Pan Sha, et al. Design of a CMOS current-adjustable charge-pump circuit insensitive to power supply and temperature. Chinese Journal of Semiconductors, 2003, 24(3): 260

[8] Ye Qiang, Lai Xinquan, Dai Guoding, et al. Design of an on-chip gate pulse modulate controller for a TFT-LCD. Journal of Semiconductors, 2008, 29(8): 1620

[9] Hoque M R, Ahmad T, McNutt T R, et al. A technique to increase the efficiency of high-voltage charge pumps. IEEE Trans Circuits Syst, 2006, 5(53): 364